Biochimica et Biophysica Acta, 731 (1983) 168–176
Elsevier

BBA 71683

KINETIC AND THERMODYNAMIC STUDIES ON NITROBENZYLTHIOINOSINE BINDING TO THE NUCLEOSIDE TRANSPORTER OF CHINESE HAMSTER OVARY CELLS *

ROBERT M. WOHLHUETER **, WAYNE ERIC BROWN and PETER G.W. PLAGEMANN

Department of Microbiology, School of Medicine, University of Minnesota, Minneapolis, MN 55455 (U.S.A.)

(Received December 13th, 1982)

Key words: Nucleoside transporter; Nitrobenzylthioinosine binding; (CHO cell)

The binding of [G-^{3}H]nitrobenzylthioinosine to intact Chinese hamster ovary cells has been studied kinetically and thermodynamically. The association of nitrobenzylthioinosine with cells is a second-order process which proceeds at 24°C with a rate constant of $2 \cdot 10^7$ $M^{-1} \cdot s^{-1}$. Dissociation of the complex was characterized as a simple first-order process with rate constant on the order of $7 \cdot 10^{-3}$ s^{-1}. The quotient of these is comparable to the dissociation constant as measured in equilibrium binding studies, $2.2 \cdot 10^{-10}$ M. The temperature dependence of the rate of association indicated an Arrhenius activation energy of 8.4 kcal·mol^{-1}, while that of the equilibrium constant for dissociation indicated a standard enthalpy change of 8.8 kcal·mol^{-1}. The large increase in affinity of nitrobenzylthioinosine as compared to natural nucleosides is attributable to an entropy-driven interaction with the binding site. Thymidine, dipyridamole and papaverine each decrease the apparent dissociation constant for the nitrobenzylthioinosine-cell complex; the latter, inhibitors of nucleoside transport, decrease the rate of dissociation of the complex.

Introduction

Nitrobenzylthioinosine (NBTI) is a potent inhibitor of nucleoside transport in several cultured mammalian cell lines as well as in erythrocytes [1]. Because of that property it protects cells in vitro against the toxic effects of nucleoside analog drugs [2], but may also enhance their efficacy by prolonging their life-time in tumor-bearing animals [3]. Experimentally, NBTI and other similar analogs of purine ribosides have found utility as titrants of nucleoside carriers in intact cells (see, for example, Refs. 4 and 5), as probes to delineate carrier specificity [6] and mechanisms [7], as high affinity ligands to aid in the isolation of carrier proteins [8], and as a means to manipulate or wholly exclude nucleoside transport [9].

The reaction which underlies this diverse utility of NBTI, namely the association of NBTI with the nucleoside carrier, has been studied chiefly from the point of view of equilibrium binding. Thus, the high affinity with which NBTI binds to cells (K_d < 1 nM) has been documented in numerous Scatchard analyses, both of radiolabeled ligand binding to cells and of the partial expression of transport inhibition. But the kinetics of association and dissociation, and the effect of temperature on these reactions have not been studied with radioactive ligand in any detail. To inform and support the experimental uses of NBTI such knowledge is essential.

In this study we address the interaction between

* A preliminary version of this work was presented at the April, 1982, meeting of the American Society of Biological Chemists, New Orleans, LA, U.S.A.

** To whom correspondence should be sent: Department of Microbiology, Mayo Memorial Building, Box 196, 420 Delaware Street, S.E., Minneapolis, MN 55455, U.S.A.

Abbreviation: NBTI, Nitrobenzylthioinosine, a trivial designation for 6([4-nitrobenzyl]thio)-9-β-D-ribofuranosylpurine.

radiolabeled NBTI and Chinese hamster ovary (CHO) cells: its kinetics, temperature dependence and relationship to other transport inhibitors.

Experimental Procedures

Cell culture. Wild-type CHO cells were grown in suspension in Eagle's minimal essential medium for suspension cultures ('MEMS', Gibco Laboratories, Grand Island, NY) supplemented (v/v) with 2% newborn calf serum, 4% calf serum, 4% horse serum and 0.53 g Pluronic F68 surfactant/liter. Cells were enumerated with a Coulter counter and checked for impermeability of trypan blue before use. For binding experiments, cells were centrifugally sedimented and resuspended at the desired cell density in basal medium ('S210', Irvine Scientific, Santa Ana, CA).

Radiolabeled nitrobenzylthioinosine. [G-^{3}H]-Nitrobenzylthioinosine was purchased from Moravek Biochemicals (lot 1720, Brea, CA), with a specific radioactivity of 17 Ci/mmol; where required, the specific radioactivity was diluted by addition of non-labeled NBTI obtained from Calbiochem (San Diego, CA). Both materials eluted together in reverse-phase HPLC (Altex Ultrasphere-ODS, 4.6 × 250 mm; isocratic elution with 1 mM P_i/NH_4^+ plus 1 mM Cl^-/NH_4^+, pH 4.8, in 55% methanol). The chromatographic analysis indicated 98% radiochemical purity for the compound as obtained from Moravek.

Equilibrium binding studies. Samples of cell suspension, generally at a final cell density of $3 \cdot 10^9$ cells/liter, were mixed with 12 concentrations (0.05 to 400 nM in geometric progression) of [^{3}H]NBTI at specific radioactivities ranging from, $3.6 \cdot 10^4$ to $1.8 \cdot 10^2$ dpm/pmol. Total volume of the mixtures was 2 ml. After incubation for > 20 min at a specified temperature, an aliquot was removed, dissolved in Triton X-114/xylene (1 : 3, v/v) containing 4 g Omnifluor/liter (New England Nuclear, Boston, MA), and assayed for radioactivity with automatic external standardization of counting efficiency (Beckman model 7500 scintillation spectrometer). Cells were separated from the mixture by brief centrifugation at 2000 × *g*, and an aliquot of the supernate assayed for tritium content.

Scintillation data were converted to concentrations of free NBTI and bound NBTI (= total minus free). Either Eqn. 1 or 2 was fitted to the binding data by non-linear least-squares regression. Eqn. 1 is a two-component binding isotherm:

$$L_b = \frac{N_1 L_f}{K_1 + L_f} + \frac{N_2 L_f}{K_2 + L_f} \quad (1)$$

where L_b = concentration of bound ligand, L_f = concentration of free ligand, N_1 and N_2 are the numbers of class 1 and class 2 binding sites per liter, and K_1 and K_2 are the macroscopic dissociation constants for class 1 and class 2 binding sites. Eqn. 2 corresponds to a single, saturable binding site plus a non-specific binding component:

$$L_b = \frac{N_1 L_f}{K_1 + L_f} + k' L_f \quad (2)$$

where k' is a linear coefficient for non-specific binding, and the other symbols are as defined for Eqn. 1.

Fits on Eqn. 1 rarely converged to satisfactory values for N_2 and K_2; when they did, the values were very high ($> 10^4$ M) and contained large standard errors. This behavior justified our routine use of Eqn. 2 to analyze binding data. In either case, the effect of including a second term is to correct the first term (representing the high-affinity site) for non-specific binding. The correction was always minor; typically 4% of total binding was attributable to the non-specific component at a concentration of ligand that supported 90% saturation of the high-affinity site (see, for example, Fig. 1C).

Rates of association and dissociation. From previous studies [6,9] it was obvious that NBTI associated rapidly with cells. We therefore adapted the rapid sampling technique we employ for nucleoside transport studies [10] to measure NBTI association with cells. Briefly, a cell suspension at stipulated cell density and temperature is mixed with a solution of [^{3}H]NBTI in volume ratio 7.3 : 1 by a dual syringe apparatus. Twelve mixed samples are delivered in timed sequence to centrifuge tubes containing 200 µl of silicone oil (density = 1.035 $g \cdot ml^{-1}$) and mounted in the rotor of the Eppendorf centrifuge. The centrifuge is started directly after the last delivery, and the cells are sedimented below the oil surface within 2 s. Extracellular and intracellular water spaces were de-

termined by [^{14}C]inulin and $^{3}H_2O$ measurements as described previously [10].

The cell-associated radioactivity includes also non-bound NBTI, distributed initially only in the extracellular space, but finally throughout the entire water space of the pellet. We have adjusted the origin of our plots to exclude that amount of tritium initially attributable to the extracellular space.

Measurement of dissociation rates were facilitated by introducing at zero-time a large excess (10^4-fold) of non-labeled NBTI to cells equilibrated with [^{3}H]NBTI; labeled NBTI dissociating from a binding site is diluted by unlabeled NBTI, so that reassociation of a labeled molecule is highly unlikely. Samples were withdrawn by pipette periodically after addition of unlabeled NBTI, spun through silicone oil, and assayed for remaining (= cell-associated) radioactivity. There are two systematic, but relatively inconsequential, errors inherent in this methodology. (1) It does not consider the contribution of non-specifically bound NBTI; as noted above this contribution was low (< 5%) and has been neglected. (2) Cells centrifuged through silicone oil carry a certain amount of extracellular water with them (typically about 10% of total pellet volume, see Ref. 10). Thus, some radioactivity recovered in the pellet is, in fact, not cell-associated, and gives rise to non-zero asymptotes in dissociation experiments. This problem is accommodated by adding a constant term to the exponential equation fitted to the data. But this approach does not rigorously distinguish radioactivity not associated with the cell, from that which might be associated, but, for some reason, unexchangeable.

Data analysis. Theoretical equations describing exponential rate laws, binding isotherms or straight lines were fitted to data by a generalized least-squares regression program based on the algorithm of Dietrich and Rothmann [11] and implemented on a Hewlett-Packard 9825 computer. Parameter values obtained by least-squares fits are reported ± the standard error of the estimate.

Results

Association / dissociation of NBTI and its equilibrium binding

Examples of association and dissociation rate measurements and of equilibrium binding analysis are presented in Fig. 1. In the case of association (panel A), the measurements were extended until equilibrium was attained. For routine purposes only 12 time points within the first twenty seconds were collected. Even in this time interval deviation from an initial, linear reaction rate was obvious and graphical estimation of initial rate was problematic. Therefore, we have fit a smooth curve to association rate data, namely $y_t = y_\infty(1 - e^{-kt})$, and report its derivative at $t = 0$, $(dy/dt)_{t=0} = ky$, as the initial rate of association. Our use of this equation is empirical and does not imply that a first-order rate law adequately describes association rate data (see below).

In the case of dissociation rate, we have also measured initial velocities as the zero-time derivative of an exponential curve, namely $y_t = (y_0 + b)e^{-kt} + b$, where b accomodates a non-zero asymptote as described above. This equation does correspond to our hypothesis that dissociation of the NBTI-cell complex is a first-order process, and we regard the many instances where it describes dissociation rate data well (exemplified in Figs. 3 and 4, and in many dissociation curves not shown) as confirmation of that hypothesis.

Panel C of Fig. 1 exemplifies equilibrium binding of NBTI to intact CHO cells at 24°C. In this example, $K_d = 1.8 \cdot 10^{-10}$ M and N_b corresponds to $3.6 \cdot 10^5$ sites per cell. The low-affinity component accounts for 4.1% of total binding at a NBTI concentration where the high-affinity site is 90% saturated. In the course of these studies, we have measured binding in 16 experiments under conditions comparable to these. Mean value ± S.E. for K_d was $(2.17 \pm 0.20) \cdot 10^{-10}$ M and mean number of binding sites per cell (± S.E.) was $(3.32 \pm 0.23) \cdot 10^5$.

Our expectation was that association would follow a second-order rate law, with velocity proportional to both NBTI concentration and to the binding-site concentration. That expectation is borne out by the data of Fig. 2. The initial rates of association were determined as in the experiment of Fig. 1A, but with NBTI and cell concentrations varied in turn. The rate of association is seen to be proportional to both. Taking $2.26 \cdot 10^5$ binding sites per cell, as measured by Scatchard analysis with this batch of cells, one calculates about the

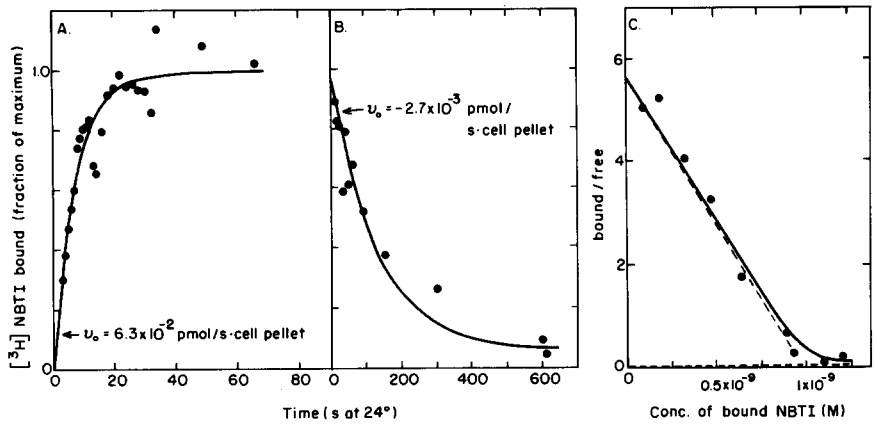

Fig. 1. Examples of the kinetics of association of [^{3}H]NBTI with CHO cells, of dissociation of the complex, and of the extent of binding at equilibrium. Panel A. A suspension of CHO cells ($3.18 \cdot 10^6$ cells per ml) was mixed with [G-^{3}H]NBTI (final concentration 5.3 nM) by means of the syringe apparatus as described in Experimental Procedures. Solutions and apparatus were at ambient temperature, 24°C. Initial velocity, υ_o, is taken as the zero-time slope of an equation of the form $y_t = y_\infty(1 - e^{-kt})$ best-fitting the time course of appearance of cell-associated radioactivity; standard error of the estimate was $5.9 \cdot 10^{-3}$. Panel B . A cell suspension ($1.3 \cdot 10^7$ cells per ml) was preincubated with [^{3}H]NBTI, total final concentration = 5 nM. At the times indicated on the abscissa the cells were diluted 8-fold into an excess (5 μM) of unlabeled NBTI. An equation for first-order decay was fitted to the data, see text, and the zero-time slope taken as initial velocity; standard error of the estimate was $1.0 \cdot 10^{-3}$. Panel C. Equilibrium binding of [^{3}H]NBTI to CHO cells ($1.65 \cdot 10^9$ cells per liter) was measured at concentrations of total NBTI from 0.2 to 100 μM at 24°C. The higher concentrations are omitted from this plot in order to expand the high-affinity component; they were, however, included in the regression on Eqn. 2. Best-fitting parameters (± S.E.) were $K_1 = (1.76 \pm 0.43) \cdot 10^{-10}$ M, $N_1 = (9.86 \pm 0.87) \cdot 10^{-10}$ M and $k' = (2.35 \pm 1.3) \cdot 10^{-2}$. The binding components corresponding to the first and second terms of Eqn. 2 were separated graphically (dotted lines) as described by Weder et al. [25]. The number of binding sites per cell computes to $3.6 \cdot 10^5$.

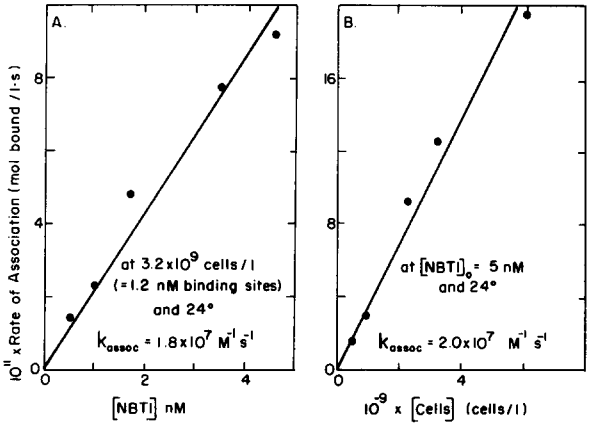

Fig. 2. Reaction order of NBTI association with CHO cells. In experiments like the one illustrated in Fig. 1A (but with only 12 time points), the rate of association of [^{3}H]NBTI with cells was measured. In panel A the cell concentration was held constant and the NBTI concentration varied as indicated on the abscissa. In panel B, total NBTI concentration was held constant and the number of cells varied. Second-order rate constants were calculated from the slopes of the lines and the number of high-affinity binding sites for these cells as measured by equilibrium binding analysis as described in Experimental Procedures.

same second-order rate constant (at 24°C) from both experiments, $1.8 \cdot 10^7$ $M^{-1} \cdot s^{-1}$ and $2.0 \cdot 10^7$ $M^{-1} \cdot s^{-1}$, respectively.

Assuming a simple ligand-protein binding model, the product of the rate constant for association (at 24°C) and the equilibrium constant for dissociation ($2.2 \cdot 10^{-10}$ M at 24°C, cf. Fig. 1C).

$$k_d \times k_{assoc} = 4.2 \cdot 10^{-3}\ s^{-1} = 0.25\ min^{-1}$$

implies a rate constant for dissociation, k_{dissoc}, which is comparable to that measured here directly (e.g. from Fig. 1B, $k_{dissoc} = 0.52\ min^{-1}$). In fact, we have seen considerable variation in dissociation rate constants from batch to batch of cells (0.27 to 0.75 min^{-1}; cf. Figs. 1, 3, and 4), more so than would be expected from the relative constancy of K_d estimates (see above). The reasons for this variability are not apparent to us.

Eilam and Cabantchik [12] have measured a second-order rate constant of $1.3 \cdot 10^8$ $M^{-1} \cdot s^{-1}$ for NBTI binding to hamster cells, based on the

fractional appearance of inhibition of uridine uptake in MTC hamster cells. We have previously measured a rate of appearance of inhibition of thymidine transport in CHO cells which calculates to a rate constant of $2.6 \cdot 10^7\ M^{-1} \cdot s^{-1}$ [6].

Temperature dependence of NBTI binding

The second-order rate constant for NBTI association with CHO cells was determined at a series of 14 temperatures, and evaluated by means of an Arrhenius plot (not shown). The curve was linear throughout the temperature range employed (0 to 40°C); from its slope an activation energy, E_a, of 8.4 kcal/mol (0.6 standard error of the estimate) is calculated. This is less than half the E_a characteristic of nucleoside transport (E_a for thymidine transport in Novikoff rat hepatoma cells = 18.3 kcal/mol, cf. Ref. 13).

The equilibrium constant for dissociation was measured at nine temperatures spanning a similar range, and the data were evaluated by means of a Van't Hoff plot (not shown). The number of binding sites was invariant with temperature. The values for $\ln K_d$ were inversely proportional to the absolute temperature and yielded an estimate of the standard enthalpy change of 8.8 ± 1.7 kcal/mol (mean ± S.E.) for the dissociation reaction.

These data support an estimate of entropy of the interaction at 24°C:

$$\Delta G^\circ = -RT \ln K_d = 13.1\ \text{kcal} \cdot \text{mol}^{-1}$$

$$\Delta S^\circ = (\Delta H^\circ - \Delta G^\circ)/T = 14.6\ \text{cal} \cdot \text{K}^{-1} \cdot \text{mol}^{-1}$$

That is, about 1/3 of the standard free energy change of the binding reaction is accounted for by the entropy component.

NBTI binding in the presence of thymidine

Thymidine was chosen as a typical, well-characterized substrate for the nucleoside carrier of CHO cells. Its Michaelis-Menten constant for zero-*trans* entry is about 100 μM [13] and its transport is inhibited > 90% by NBTI [6].

We ran equilibrium binding analyses of NBTI (at 24°C) in the presence of 0, 100, 300 and 900 μM thymidine. The measured apparent dissociation constants, K_d, are listed in Table I. These values vary linearly with the concentration of thymidine and extrapolate to an inhibition constant for thymidine of 142 μM. There is some uncertainty in the actual thymidine concentrations attained in this experiment, since thymidine is phosphorylated by CHO cells. The extent of phosphorylation was minimized by completing the experiments within 2 min exposure time to thymidine; this time should still be sufficient to allow NBTI binding to come to equilibrium (cf. Fig. 1A). Under the conditions employed, it is unlikely that more than a few percent of the total thymidine would have been phosphorylated (cf. Ref. 14).

In Fig. 1B it was illustrated how the presence of unlabeled NBTI 1000-fold excess, corresponding to 10^5 times the K_d value) facilitated measurement of NBTI dissociation by preventing the reassociation of labeled NBTI. A similar effect could be obtained by presenting thymidine to the NBTI cell complex at sufficiently high concentration, as illustrated in Fig. 3. At the lower concentration of

TABLE I

THE EQUILIBRIUM CONSTANT WAS DETERMINED AS DESCRIBED IN EXPERIMENTAL PROCEDURES AT 24°C

Cell suspensions were preincubated with test compound about 2 min prior to addition of [^{3}H]NBTI, which was allowed to equilibrate a further 40 min before assay. The number of binding sites per cell were essentially invariant within each experiment.

Test compound	Concentration (μM)	Dissociation constant (M) ($\times 10^{10}$)
Thymidine	0	1.3
	100	2.7
	300	4.6
	900	9.5
Dipyridamole	0	2.2
	0.05	3.9
	0.1	5.7
	0.2	9.0
	0.5	14.9
Papaverine	0	1.6
	1.0	2.0
	2.5	1.8
	5.0	2.8
	10	4.6
	25	6.9

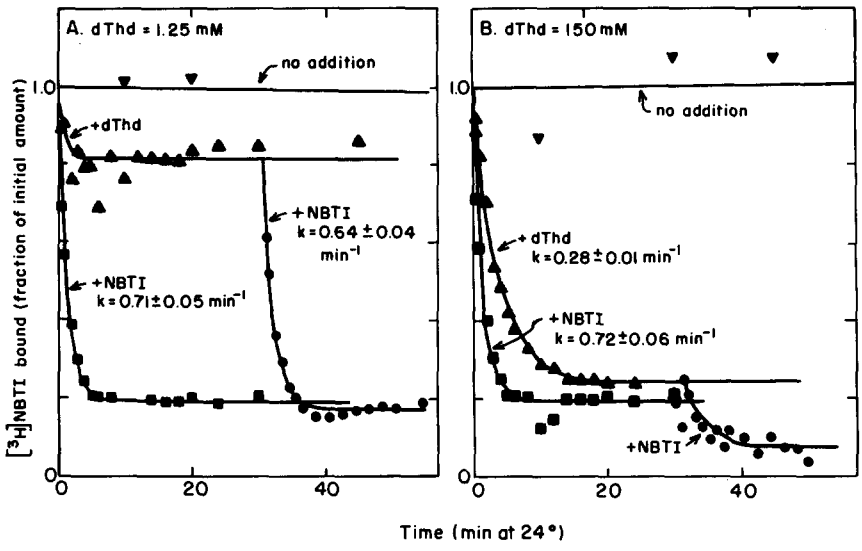

Fig. 3. The effect of thymidine on the kinetics of dissociation of NBTI-cell complex. Suspension of CHO cells, $1.7 \cdot 10^7$ cells per ml, was incubated with [^{3}H]NBTI, final total concentration = 7.5 nM. The suspension was divided into three portions. At zero-time, one portion received no addition (▼), a second portion (+NBTI, ■) received unlabeled NBTI at a final concentration of 5.0 μM, a third portion received thymidine (+dThd, ▲) at a final concentration of 1.2 mM (panel A) or 150 mM (panel B). The third portion was later subdivided, and one part of it received unlabeled NBTI (+NBTI, ●) at a final concentration of 5.0 μM. 500 μl samples of each portion were periodically withdrawn, the cells centrifuged through silicone oil, and the pellet analyzed for tritium. Samples of control (▼) taken at 60 and 75 min are not shown. First-order decay constants were calculated by least squares regression for each reaction mixture, as noted on the figure.

thymidine (1.2 mM corresponding to 12 times the K_m value; panel A) displacement of labeled NBTI was about 20%. When excess unlabeled NBTI was added after attainment of binding equilibrium in the presence of thymidine, the rate constant for dissociation of [^{3}H]NBTI was about equal to that observed in the absence of thymidine. At the higher concentration of thymidine (150 mM corresponding to 1500 times the K_m value; panel B) displacement was 90% of the maximal displacement seen in the presence of both NBTI and thymidine. The apparent rate of dissociation of [^{3}H]NBTI for the cells in the presence of thymidine was less than half that seen when unlabeled NBTI was used to prevent reassociation of labeled NBTI.

NBTI binding in the presence of other transport inhibitors

The foregoing experiments with thymidine were predicated on the assumption that NBTI and thymidine bind to the same site on the carrier. Dipyridamole and papaverine are compounds known to inhibit the transport of nucleosides in various cell types [7,15,16,17], and also of other compounds thought not to be transported by the nucleoside system [18]. Equilibrium binding and dissociation kinetic studies analogous to those done with thymidine were also conducted with these compounds.

The apparent K_d for [^{3}H]NBTI binding in the presence of various concentrations of these inhibitors is given in Table I. Plots of these data (not shown) are linear, permitting definition of K_i values of 0.17 μM for dipyridamole and 7.2 μM for papaverine. The results with dipyridamole are qualitatively similar to those reported by Paterson et al. [17] for NBTI binding to HeLa cells. The mode and potency of inhibition by dipyridamole and papaverine of nucleoside transport in CHO cells has not yet been established.

The effects of dipyridamole and papaverine on the dissociation kinetics of NBTI-cell complex are depicted in Fig. 4, panels A and B, respectively. Cell suspensions preincubated with [^{3}H]NBTI were either exposed to the test compound or not, and

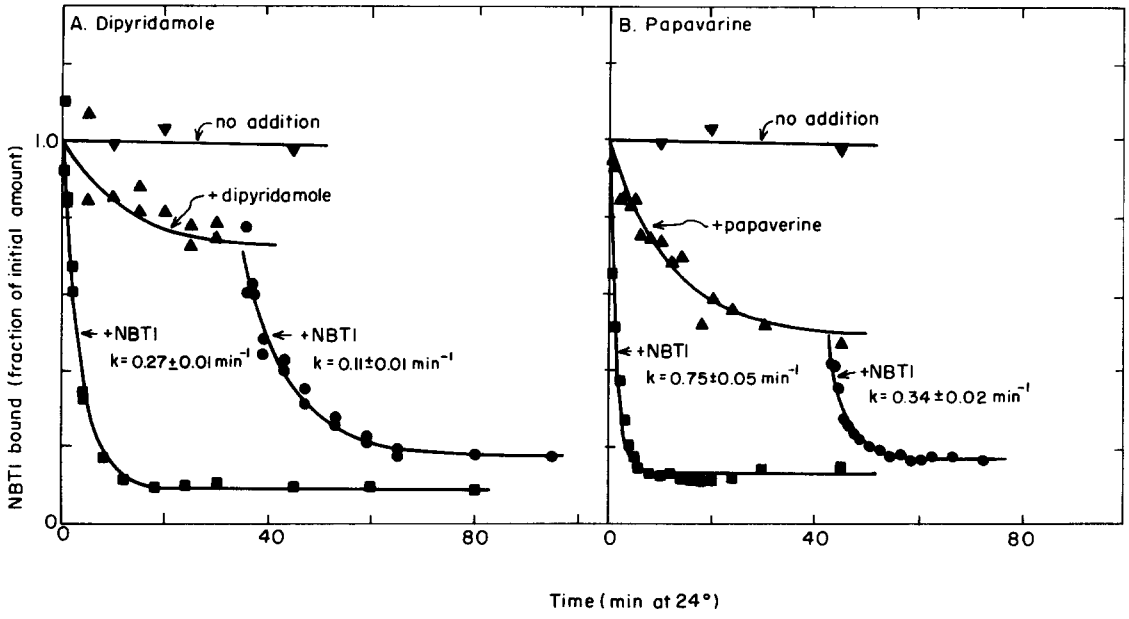

Fig. 4. The effects of dipyridamole and papaverine on the kinetics of dissociation of NBTI-cell complex. The experiments were carried out at an ambient temperature of 24°C according to a protocol similar to that described in the legend to Fig. 3. In panel A, the initial cell suspension was $7.1 \cdot 10^6$ cells per ml and contained 0.6 nM [^{3}H]NBTI. Dipyridamole was added at a final concentration of 40 μM. In panel B, the initial cell suspension was $1.1 \cdot 10^7$ cells per ml and contained 1.5 nM [^{3}H]NBTI. Papaverine was added at a final concentration of 250 μM.

then the dissociation of labeled NBTI was monitored after addition of a large excess of unlabeled NBTI. The first-order dissociation rate constants in each case were calculated by least-squares regression and are noted in the figure. 40 μM dipyridamole reduced the rate of NBTI-cell dissociation by 60%, 250 μM papaverine by 55%.

Discussion

The data presented here support the view that the binding of NBTI to its high-affinity sites on CHO cells is a typical, well-behaved case of ligand-protein binding, albeit with a remarkably high affinity. Equilibrium binding analysis shows a single high-affinity component, as observed also by many other investigators. Association of [^{3}H]NBTI with cells follows a straightforward, second-order rate law (Fig. 2), with a rate constant typical for the interaction of small ligands with enzymes. Fersht (Ref. 19, Table 4.3) provides a handy compilation for comparison.

Dissociation, too, seems straightforward; it can be described as first-order decay (cf. Figs. 1B, 3 and 4). The first-order rate constant for dissociation is lower than that typically observed for ligand-enzyme dissociation [19], consistent with an extraordinarily low K_d for the NBTI binding reaction. The kinetic measurements agree reasonably well with the equilibrium measurements, i.e. $k_{dissoc}/k_{assoc} \simeq K_d$.

There is little doubt that the high-affinity binding of NBTI is to the nucleoside carrier. This conclusion is demonstrated most convincingly by the excellent correlations between NBTI binding sites and nucleoside transport activity reported by Jarvis [20] and Cass et al. [5]. It is corroborated and extended in the present work by the demonstration (Fig. 3) that thymidine occupies sites vacated by [^{3}H]NBTI, that thymidine increases the apparent K_d for NBTI in a competitive fashion, and by agreement between the rate of association as measured here with [^{3}H]NBTI and that estimated by us previously [6] on the basis of the rate of appearance of the inhibitory effect. These observations are all consistent with the notion that

NBTI binds to a site on the nucleoside carrier which also binds thymidine. We presume that site is strategically involved in thymidine transport.

The simple ligand-protein model is supported also by the results of the temperature-dependence studies. Over the temperature range 0 to 40°C, the second-order rate constants of association generated a linear Arrhenius plot with no indication that possible membrane phase-transitions influence association rates. The activation energy corresponded to a Q_{10} (24 to 34°C) of about 1.6, which is low relative to those typical of covalent reactions or reactions involving protein conformational shifts. By way of comparison, the Q_{10} for thymidine transport in Novikoff rat hepatoma cells, a process presumably involving conformational shift of the carrier protein, is 2.7 [13].

It is obvious from structural considerations that the presence of the lipophilic nitrobenzyl group is responsible for an approximately 10^6-fold gain in affinity (K_d for NBTI $\simeq 2 \cdot 10^{-10}$ M; K_m for inosine transport is likely on the order of 10^{-4} M; cf. Ref. 21). Drawing again on a comparison to the thermodynamically well-characterized case of thymidine transport in Novikoff cells, we see that the enthalpies of NBTI binding and thymidine binding are comparable (8.8 kcal $\cdot$ mol^{-1} and 9.3 kcal $\cdot$ mol^{-1}, respectively). NBTI binding, however, is accompanied by a positive change in entropy (15 cal $\cdot$ K^{-1} $\cdot$ mol^{-1}), thymidine binding is accompanied by a negative change in entropy (-15 cal $\cdot$K^{-1} $\cdot$ mol^{-1}). Thus, the difference in $\Delta G°$ of the reaction of benzylated nucleosides relative to that of natural nucleosides is entirely attributable to an entropy-driven interaction of the benzyl moiety with the binding site of the carrier. The conclusion reminds us of the observation of Krupka and Deves [22] that increasingly long aliphatic additions to the choline molecule endow the analogs with increasingly higher affinity for the choline transporter.

Assuming that nucleoside transport is kinetically symmetrical in CHO cells as we know it to be in HeLa and Novikoff rat hepatoma cells [23], the nucleoside binding site of the carriers in the absence of ligand should be equally distributed between inward- and outward-facing orientations. We might have expected, therefore, to detect two kinetically distinguishable classes of binding sites corresponding to these two orientations, but only one thermodynamic class. In none of the kinetic experiments was more than one class of site discernable. This implies either (i) that carrier reorientation is sufficiently fast as to be invisible at the time scale of NBTI binding, or (ii) that the membrane bilayer, which establishes the two orientations of carrier, is a negligible barrier to NBTI diffusion towards its binding sites, or both.

The rate of carrier reorientation can be estimated from the maximum velocity of nucleoside transport and the number of carriers per cell: for $V_{max} = 4.6$ μM $\cdot$ s^{-1} [21], $3.3 \cdot 10^5$ sites per cell (present paper) and approx. 1 μl of cell water per 10^6 cells, a turnover of 8.4 s^{-1} is calculated. (In a previous paper we estimated 31 s^{-1} for CHO cells [6]; recently Jarvis et al. [9] have estimated 192 s^{-1} for erythrocytes from sheep.) Thus, at 24°C, a given carrier reorients about every 60 ms.

The diffusion of NBTI across the cell membrane can be estimated from its lipophilicity as gauged by its partition between octanol and water [24]. The quotient of rate constant for non-mediated permeation divided by the partition coefficient is constant over a wide range of partition coefficients [21], viz. 0.03 s^{-1}. The octanol/water partition coefficient for [^{3}H]NBTI is 30 (unpublished results); this indicates that the first-order rate constant for the attainment of equilibrium across the membrane should be about 0.9 s^{-1}. That is, NBTI, at any concentration, can be expected to attain 90% of equilibrium across the cell membrane in 2.5 s. The actual rate of diffusion of NBTI into the cell interior is difficult to assess. At 5 μM NBTI, at which concentration specific binding to the nucleoside carrier is negligible, a steady-state level of cell-associated NBTI is established by the earliest time we are able to measure, 2.2 s (data not shown). That level is about 9-times the concentration expected if NBTI were merely to equilibrate with intracellular water.

Considering the time scales of carrier reorientation and NBTI equilibration, it is clear that under our reaction conditions and with our methodology, we could not expect to distinguish kinetically two different orientations of the carrier.

In contrast to the apparent mechanistic simplicity of NBTI inhibition of nucleoside transport, the mechanism by which dipyridamole and papaverine inhibit is perplexing.

On the one hand, there are good reasons to think that these compounds are not specific competitors for the nucleoside binding site: (i) It is difficult to see a structural analogy to nucleosides. (ii) Dipyridamole shows non-competitive inhibition of uridine transport in rat hepatoma cells [16]. (iii) Both compounds are known to inhibit the uptake of compounds whose transport is not mediated by the nucleoside carrier (e.g. nucleobases, hexoses, choline [15]), and even of compounds whose permeation appears to be non-mediated (e.g. cytosine and L-glucose [18]). According to this view, inhibition of a given transporter results from some fairly general perturbation of the membrane.

On the other hand, both compounds seem to compete with NBTI for the NBTI binding site (Table I), an observation reported also by Paterson et al. [17] for dipyridamole inhibition of NBTI binding to HeLa cells. (It should be noted, however, that the interpretation of a competitive relationship, and particularly of the value computed for K_i, rests on the implicit assumption that the test compound binds only to the common binding site, an untested and probably invalid assumption.)

Of the present data, perhaps the experiments of Fig. 4 bear most incisively on the question of the mode of interaction of dipyridamole and papaverine with the nucleoside transporter. With both substances a perturbation of the [^{3}H]NBTI/cell equilibrium, qualitatively consistent with their effects on K_d (see Table I), is evident. However, in both cases also, the subsequent rate of dissociation of NBTI-cell complex, as measured in the presence of excess unlabeled NBTI, is much slower than that in the absence of these inhibitors. Such a reduction in the rate constant of dissociation cannot be reconciled with a merely competitive ligand. Interference with ligand-carrier dissociation might, however, be caused by an interference with carrier reorientation, or even with the rate of diffusion of [^{3}H]NBTI released inside the cell to the outside. As explained above, dipyridamole and papaverine have been implicated in just such interferences.

Acknowledgement

This study was supported by USPHS grant GM24468.

References

1 Paterson, A.R.P. and Oliver, J.M. (1971) Can. J. Biochem. 49, 271–274
2 Paterson, A.R.P., Paran, J.H., Yang, S.-E. and Lynch, T.P. (1979) Cancer Res. 39, 3607–3611
3 Paterson, A.R.P., Jakobs, E.S., Harley, E.R., Fu, N.-W., Robins, M.J. and Cass, C.E. (1983) in International Symposium on Adenosine (Berne, R.M. and Rubio, R., eds.), Martinus Nijhoff, The Hague, in the press
4 Jarvis, S.M. and Young, J.D. (1980) Biochem. J. 190, 377–383
5 Cass, C.E., Kolassa, N., Uehara, Y., Dahlig-Harley, E., Harley, E.R. and Paterson, A.R.P. (1981) Biochim. Biophys. Acta 649, 769–777
6 Wohlhueter, R.M., Marz, R. and Plagemann, P.G.W. (1978) J. Membrane Biol. 42, 247–264
7 Jarvis, S.M., McBride, D. and Young, J.D. (1982) J. Physiol. 324, 31–46
8 Jarvis, S.M. and Young, J.D. (1981) Biochem. J. 194, 331–339
9 Harley, E.R., Paterson, A.R.P. and Cass, C.E. (1982) Cancer Res. 42, 1289–1295
10 Wohlhueter, R.M., Marz, R., Graff, J.C. and Plagemann, P.G.W. (1978) Methods Cell Biol. 20, 211–236
11 Dietrich, O.W. and Rothmann, O.S. (1975) Keyboard (Hewlett-Packard) 7, 4–7
12 Eilam, Y. and Cabantchik, Z.I. (1977) J. Cell. Physiol. 92, 185–202
13 Wohlhueter, R.M., Marz, R. and Plagemann, P.G.W. (1979) Biochim. Biophys. Acta 553, 262–283
14 Marz, R., Wohlhueter, R.M. and Plagemann, P.G.W. (1977) J. Supramol. Struct. 6, 433–440
15 Plagemann, P.G.W. and Richey, D.P. (1974) Biochim. Biophys. Acta 344, 263–305
16 Plagemann, P.G.W., Marz, R. and Wohlhueter, R.M. (1978) J. Cell. Physiol. 97, 49–72
17 Paterson, A.R.P., Lau, E.Y., Dahlig, E. and Cass, C.E. (1980) Mol. Pharmacol. 18, 40–44
18 Graff, J.C., Wohlhueter, R.M. and Plagemann, P.G.W. (1977) J. Biol. Chem. 252, 4185–4190
19 Fersht, A. (1977) Enzyme Structure and Function, W.H. Freeman and Co., San Francisco
20 Jarvis, S.M. (1983) in International Symposium on Adenosine, (Berne, R.M. and Rubio, R. eds.), Martinus Nijhoff, The Hague Abstr. No. 10 in the press
21 Plagemann, P.G.W. and Wohlhueter, R.M. (1980) Curr. Top. Membranes Transp. 14, 225–330
22 Krupka, R.M. and Deves, R. (1980) J. Biol. Chem. 255, 8546–8549
23 Wohlhueter, R.M. and Plagemann, P.G.W. (1982) Biochim. Biophys. Acta 689, 249–260
24 Lieb, W.R. and Stein, W.D. (1971) Curr. Top. Membranes Transp. 2, 1–39
25 Weder, H.G., Schildknecht, J., Lutz, R.A. and Kesselring, P. (1974) Eur. J. Biochim. 42, 475–481